Garcia-Pardo, C.; Andreu-Estellés, C.; Fornés Leal, A.; Castelló-Palacios, S.; Pérez-Simbor, S.; Barbi, M.; Vallés Lluch, A.... (2018). Ultrawideband Technology for Medical In-Body Sensor Networks: An Overview of the Human Body as a Propagation Medium, Phantoms, and Approaches for Propagation Analysis. IEEE Antennas and Propagation Magazine. 60(3):19-33. doi:10.1109/MAP.2018.2818458

UWB Propagation Environment for Medical In-Body Sensor Networks

Concepcion Garcia-Pardo, Carlos Andreu, Alejandro Fornes-Leal, Sergio Castelló-Palacios, Sofia Perez-Simbor, Martina Barbi, Ana Vallés-Lluch, and Narcis Cardona, *Member*, *IEEE*

***Abstract* —In-body sensor networks are those networks where at least one of the sensors is located inside the human body. Such wireless in-body sensors are mainly used for medical applications, collecting and monitoring important parameters for health and diseases treatment. The IEEE Standard 802.15.6-2012 for Wireless Body Area Networks (WBAN) considers in-body communications in the Medical Implant Communication Service (MICS) band. Nevertheless, high data rate communications are not feasible at the MICS band due to its narrow occupied bandwidth. In this framework, Ultra-Wideband (UWB) systems have emerged as a potential solution for in-body high data rate communications, due to its miniaturization capabilities or low power consumption. In the last years, some open issues have determined the research about in-body propagation. Firstly, the propagation medium, i.e., the human body tissues, is frequency-dependent and exhibits a large attenuation at UWB frequencies. Secondly, the behavior of the in-body antennas is highly dominated by the surrounding tissues. Thus, the in-body channel characterization in UWB depends not only on the channel behavior itself, but also on the methodology of characterization. This paper intends to outline the research performed in the field of UWB in-body radio channel characterization considering the propagation medium, as well as the methodology of analysis – software simulations, phantom measurements, *in vivo* measurements–. Thus, authors provide an overall perspective of the current state of the art, limitations for the analysis of in-body propagation, and future perspectives for UWB in-body channel analysis.**

***Index Terms*—In-body, phantoms, body tissues, Body Area Networks (BAN), Ultra-Wideband (UWB), path loss models.**

I. Introduction

THE use of wireless technologies in medical devices has increased considerably in the last years. Significant advances in microelectronics have enabled the integration of biomedical sensors and radio transceivers into wearable and implantable wireless sensors [1]. Such devices collect and monitor key physiological data from the patient and send them to a remote node located either inside the human body, over or away from the surface of the body [2]. Intraocular pressure sensors for glaucoma monitoring [3], cardiac implants such as pacemakers or implantable cardioverter defibrillators (ICD) [4], Electromyogram (EMG) sensors for controlling active prostheses [5], wireless capsule endoscope for video recording of the bowel [6], or brain machine interface (BMI) sensors for monitoring the neural activity of the brain [7] are only some examples of different applications and uses of wireless implanted sensors for medical purposes.

In the literature, different technologies have been addressed for implant communications such as optical [8], ultrasounds [9] or radiofrequency [10]. Most of them are based on the radiation and propagation of signals through the body so that the influence of the different body tissues and the corporal fluids should be taken into account. Some other technologies such as graphene magneto resonance [11] have recently tried to overcome these issues although they are still under investigation.

The technical requirements of radiofrequency medical devices are strongly influenced by the in-body scenario of application. In particular, such medical in-body devices are restricted in terms of required data rate and therefore in terms of bandwidth. Thus, different frequency bands have been used for in-body medical devices. The IEEE Standard 802.15.6-2012 for Wireless Body Area Networks (WBAN) allocates the different frequency bands of the electromagnetic spectrum to the operation of implantable or wearable sensors [12]. The Medical Implant Communication Service (MICS) band, which operates from 402 to 405 MHz, was initially allocated for communications between an in-body sensor and other sensor located either inside, over or out of the body surface [13], [14]. The main advantage of this frequency band is its good propagation conditions over the different body tissues [15]. However, its 3 MHz bandwidth, which is by far insufficient for high data rate communications, is its main drawback [16]. The standard also envisioned the use of the Industrial, Scientific and Medical (ISM) radio band (2400-2483.5 MHz) for communications between on-body nodes and either on-body or off-body nodes. This frequency band has been also considered for in-body communications in different works in the literature [17]–[20]. Nevertheless, this band is currently overloaded due to the operation of WPAN and WLAN communications so medical devices could be interfered by other commercial wireless systems [21]. Besides, communications at this frequency band are not able to reach the data rates provided by current wireless technologies [22].

This work was supported by the Programa de Ayudas de Investigación y Desarrollo (PAID-01-16) from Universitat Politècnica de València, and by the Ministerio de Economía y Competitividad, Spain (TEC2014-60258-C2-1-R), by the European FEDER funds. This work was also funded by the European Union's H2020:MSCA:ITN program for the "Wireless In-body Environment Communication- WiBEC" project under the grant agreement no. 675353.

C. Garcia-Pardo, C. Andreu, A. Fornes-Leal, S. Castelló-Palacios, S. Pérez-Simbor, M. Barbi and N. Cardona are with iTEAM, Universitat Politècnica de València, 46022 Valencia, Spain (e-mail: {cgpardo, caranes, alforlea, sercaspa, sopresim, marbar6, ncardona}@iteam.upv.es).

S. Castelló-Palacios and A. Vallés-Lluch are with the Centre for Biomaterials and Tissue Engineering, Universitat Politècnica de València, 46022 Valencia, Spain (email: sercaspa@iteam.upv.es, avalles@ter.upv.es).

During the last decade, the Ultra-Wideband (UWB) frequency band has been investigated for short-range high data rate communications [23]. UWB signals can operate between 3.1 GHz and 10.6 GHz, occupying a minimum bandwidth of 500 MHz (absolute bandwidth) or the 20% of its carrier frequency (relative bandwidth). In the case of WBAN, this band was initially envisioned for wearables (on-body) devices [12]. Nonetheless, its multiple advantages, such as low power consumption and antenna miniaturization, have led it to be considered as a good candidate for in-body high data rate communications [24]–[27]. For example, cortical implants [27], and novel wireless capsule endoscope [28], have been addressed in the literature to benefit from this technology.

The main weakness of UWB systems for in-body communications is the large attenuation suffered by UWB signals when propagating through human body tissues [29]. Such attenuation is highly influenced by the dielectric characteristics (permittivity, conductivity) of the different body tissues, which are frequency dependent [30]. Thus, the prediction of the behavior of the radio channel between transmitter and receiver is challenging [31]. Besides, it is worth mentioning that the antennas involved in a communication link play a key role, since their parameters (operating frequency band, radiation pattern, etc.) are dramatically modified in contact with the body tissues [32].

The characterization of the radio channel for in-body communications at UWB frequencies typically is accomplished under different perspectives:

- *Mathematically by means of software calculations*. In this case, precise human anatomical models are used in typical software tools for electromagnetic computation. These models emulate the shape and size of human body organs taking into account biological parameters [33], [34]. In the case of UWB frequencies, these models should have a high accuracy in the whole band; so the overall computational cost increases dramatically [35]. Furthermore, mathematical simulations cannot replicate the physiological behavior of corporal processes such as metabolism, breathing, heart beating or blood flow [36].
- *Experimentally by means of measurements in realistic conditions*. Hence, the propagation medium (human body tissues) should be accessible. Experimental measurements for exploring in-body propagation can be classified as follows:
  - Laboratory measurements. These kinds of measurements use chemical compounds (also known as phantoms) that replicate the dielectric properties of the human body tissues involved in the considered scenario of application [37] and are more cost-effective and easier to carry out. The main drawback is the phantom, which should be tuned in the whole band under test [38]. In fact, not many UWB phantoms can follow the relative permittivity of human tissues in the entire UWB band [39]. In addition, some of them [40] exhibit a poor accuracy, leading to bad estimation of the radio channel parameters [31]. Besides, the collection of body tissues mimicked in the UWB band is highly limited, although recently the phantom formulation reported in [41] allows the imitation of several body tissues within UWB using common chemical compounds.
  - *In vivo* measurements by surgical procedures on living animals. In these kinds of experiments, pig models are usually used due to their similarity to human body tissues in terms of size and dielectric characteristics [13]. Nevertheless, many ethical constraints should be managed and measurements should be done in a surgery room in a hospital. Therefore, these kinds of measurements are complex and costly, so not much research has been carried out on living animals [36], [42]–[44].

In summary, the investigation of the UWB in-body radio channel should consider the different parts of the radio link: transmitting and receiving antennas as well as the propagation medium. As mentioned before, the propagation medium depends not only on the characteristics of the different body tissues crossed by the transmitted signal (brain tissues, torso tissues, abdomen tissues, etc.), but also on the methodology of characterization used (software, phantoms or *in vivo*). Thus, a vast collection of channel models for in-body communications can be found in the literature although they can vary dramatically with the scenario of application.

This paper aims at reviewing the characterization of the in-body radio channel at UWB frequencies considering the aspects mentioned before. To the best of our knowledge, there is no review work considering not only antennas and radio channel, but also the methodology of analysis, i.e., the kind of emulation of the propagation medium –human body tissues–. The remainder of this paper is as follows: firstly, Section II deals with the broadband characterization of body tissues in broadband, including both computer human body models for software simulations and experimental phantom models for laboratory measurements. Next, Section III provide an overview of the current state of the art of in-body channel models considering implanted and on-body antennas as well as the propagation medium. Finally, Section IV summarizes the main highlights of this work and suggests future areas of the research in in-body radio links at UWB frequencies.

II. Characterization of Body Tissues

Permittivity, conductivity and permeability characteristics describe the signal attenuation, velocity of propagation, and the range of the linear frequency effects for every propagation medium [45]. Since body tissues are non-magnetic materials, their permeability is almost the same as in free space [46]. On the contrary, both permittivity and conductivity are different between the different tissues and the air. The relative permittivity, ε_r, is a complex frequency-dependent material property defined as the absolute permittivity of such material normalized to that of the vacuum. The real part of the permittivity, $\varepsilon_r^{'}$, is the dielectric constant, and its imaginary part, $\varepsilon_r^{''}$, is the loss factor. The conductivity, σ (S/m), is also a

frequency-dependent term that comprises both the electrical losses due to ionic conductivity and those caused by the dielectric polarization, which is related to the loss factor.

The open-ended coaxial technique has been the most used method for measuring the electromagnetic properties of body tissues within UWB frequencies. It is a broadband, non-destructive method mainly used for measuring liquid and semi-solid materials. This method has been used not only to characterize biological tissues but also food [47], moisture [48] and chemical compounds and solutions [49], [50], among other applications. The system consists of a vector network analyzer (VNA) connected to an open-ended coaxial probe –a rigid coaxial cable with a flat cut end–, and a computer for processing measurements [51]. The probe has to be pressed against the tissue under test (TUT), as one can observe in Fig. 1. Then, the reflection of an electromagnetic signal in the change of medium from the probe to the TUT can be processed to extract the TUT's permittivity and conductivity.

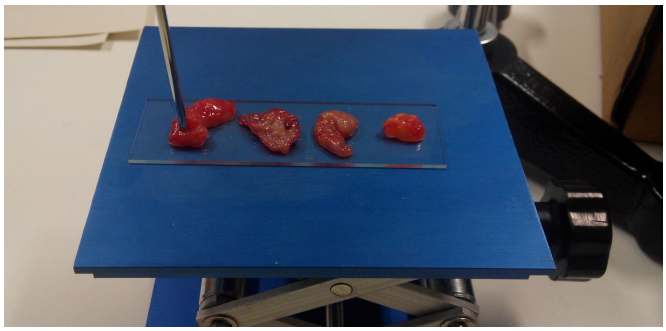

Fig. 1. Illustration of *ex vivo* colon tissue characterization [52].

There are several studies in which the electromagnetic properties of body tissues in UWB (or at least part of this band) are addressed. Measurements were performed on different frequency bands and tissues of specimens such as cats [53], sheep [30], rats [51], [54], [55], rabbits [56], cows [57], [58], dogs [59]–[61], frogs [62], swine [63], [64], mice [65], [66] and humans [52], [67]–[69]. However, these works were performed at *ex vivo* conditions, i.e., samples were analyzed some minutes or even hours after extraction. It should be noted that the electromagnetic properties of body tissues differ between *ex vivo* and *in vivo* conditions, mainly because of the tissue dehydration and ischemic effects as explained in [70]. Subject's age [54], [71], as well as the sample handling [72], temperature [58] and time from resection to measurement [69] are factors that affect the electromagnetic properties to a greater or lesser extent. Besides, there are some recent studies assessing the dielectric properties in *in vivo* conditions, although the number of available tissues is more limited. Such *in vivo* studies have reported measurements on cats [53], [73], rats [73], frogs [62], swine [74], [75], sheep [76], mice [77] and humans [78], [79].

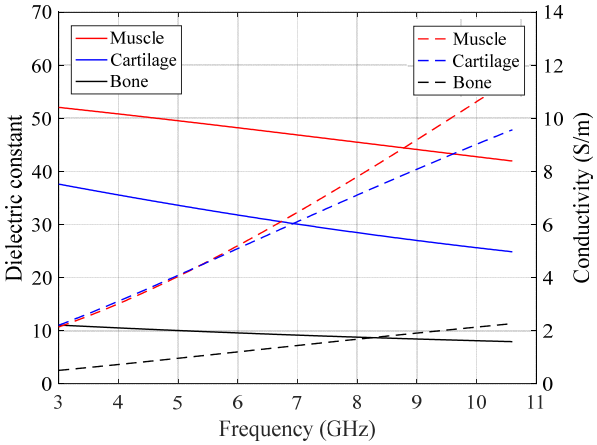

Fig. 2. Dielectric constant (solid lines) and conductivity (dashed lines) of different human tissues [30].

By analyzing the different contributions that contain UWB data, it can be easily observed that the dielectric constant is larger for high water-content tissues like muscle than for low water-content ones such as bones, as one can observe in Fig. 2. The dielectric constant decreases as frequency increases for any tissue, and its decrement is mainly due to the contribution of the dipolar relaxation of water [80], having its maximum slope in a relaxation frequency and coinciding with a maximum of the loss factor [81]. This relaxation frequency is different for each body tissue, and is principally determined by its water content. Conversely, conductivity increases with frequency and thus the signal attenuation [18].

Although the nature of the information presented in the different studies available in the literature is similar, their motivations may diverge. Some of these studies aim at investigating the difference between healthy and malignant tissues for cancer diagnosis or for improving medical applications like hyperthermia and medical imaging rather than propagation issues. For instance, the Institute of Telecommunications and Multimedia Applications (iTEAM) of the Universitat Politècnica de València has conducted a measurement campaign jointly with the Hospital Universitari i Politècnic La Fe de Valencia, with the aim of studying the differences in permittivity between healthy and malignant human colon tissue [52]. In this study, healthy and cancerous colon samples from 20 human patients were characterized. It was concluded that malignant samples have higher values of dielectric constant and conductivity for the whole UWB range. The difference in terms of dielectric constant between healthy and cancerous samples is higher at the lower part of UWB (around five points), whereas the difference in conductivity is larger at higher frequencies as one can observe in Fig. 3. Such studies open up the possibilities of including UWB signals in medical devices not just for communications but for cancer detection, diagnosis and treatment.

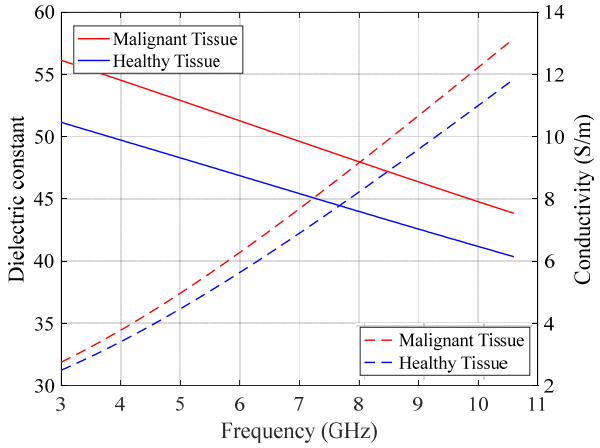

Fig. 3. Dielectric constant (solid lines) and conductivity (dashed lines) of healthy and malignant human colon tissue [52].

The dielectric data is important not only for getting a better understanding of the in-body human channel, but also for developing environments, such as software simulation tools and electromagnetic phantoms, which use these data to emulate the UWB in-body channel. Using these environments, the evaluation of the performance of antennas and systems without the need of human and animal experimentation is also possible.

A. Electromagnetic Software Emulation of Body Tissues

Several commercial electromagnetic simulation software such as CST Microwave Studio®, ANSYS HFSS™, COMSOL®, FEKO® or Sim4Life allow modelling human body tissues along with their electromagnetic properties. In these tools, one can firstly import a homogeneous model that represents a unique solid object (that can be an entire human body, a specific body region or a particular organ), heterogeneous models considering multiple tissues (see Fig. 4), poser models in which subjects have a specific position, etc. These models are obtained using or combining different techniques such as Magnetic Resonance Imaging (MRI), Computed Tomography (CT) or photography processing of sliced death corpses. Next, these models are related to their corresponding complex frequency-dependent permittivity values (one for the homogeneous models, several for the heterogeneous ones) for the working frequencies. The data reported in [30] (mainly obtained from ovine *ex vivo* specimens) are the most used for this purpose due to the huge number of tissues available, the large bandwidth of its measurements and the availability of the aforementioned fitting parameters.

Using these simulation environments jointly with the human models, it is possible to implement multiple setups of in-body propagation scenarios and thus compute the performance of different in-body UWB antennas or the propagation between them. Some of the available and most used heterogeneous models along with their corresponding spatial resolutions are presented in Table I.

TABLE I
HETEROGENEOUS HUMAN MODELS FOR ELECTROMAGNETIC SIMULATIONS

Model	Resolution (mm^3)	References
Virtual Population (Several different subjects)	0.5×0.5×0.5	[33], [82]
Visible Human Model	1×1×1 (Male) 0.33×0.33×0.33 (Female)	[34], [83]
Chinese Visible Human Project (Male and Female)	1×1×1	[84]
GSF Family (Several different subjects)	0.85×0.85×4 (best case) 2.08×2.08×8 (worst case)	[85]
Japanese Male and Female	2×2×2	[86]
Naomi (aNAtOMIcal model) and Norman (NORMAlized maN)	2×2×2	[87], [88]

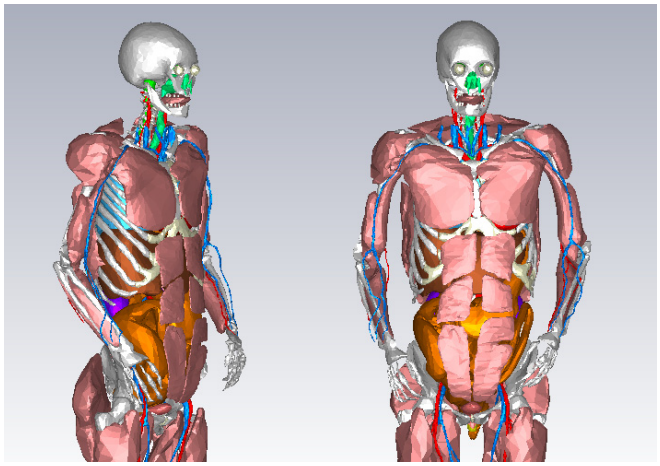

Fig. 4. Inner tissues of the CST Female Visible Human Model "Nelly" [89].

The reproduction of the human body anatomy improves as the resolution of the computer model increases. A good model resolution has an affordable cost in terms of memory and representation. Besides, a meshing of the body has to be done prior to simulation, which consists in discretizing the body into polygons (e.g., into tetrahedral or hexahedral shapes). In the resulting volumes, also known as cells, the electric and magnetic fields are computed using a numerical technique. The accuracy of the simulation can be incremented by increasing the number of cells, but this will also result in higher computational cost and time [90].

However, it is important to keep in mind that electromagnetic simulation also has some drawbacks. Since the human models have a limited resolution, there is a trade-off between simulation accuracy and computational cost. In addition, physiological processes like metabolism, breathing, heart beating or blood flow [36] are not replicated.

B. A. Experimental Tissue-Equivalent Phantoms

As mentioned before, a synthetic environment for emulating the propagation medium is needed for realistic measurements in laboratory [106]. This synthetic setting is composed of the so-called phantoms, which are materials having the same dielectric properties as those of the human tissues. Depending

TABLE II
REPORTED PHANTOMS OF DIFFERENT BODY TISSUES AND THEIR CORRESPONDING ACCURACY FOR THE UWB BAND

Tissue & Accuracy (Real Part | Imaginary Part)	Frequency Range (GHz)	Type	Components	Ref.
Muscle (5.61 | 7.06) (Accuracy in RMSE*)	3.1 – 10.6	L	Water, Sucrose	[40]
Breast (Normal, 3 types, 0.5-6 GHz: 1.59/1.90/0.54 | 0.45/0.83/0.14; 6-12 GHz: 0.53/3.79/0.31 | 1.12/1.60/0.16), Malignant (0.5-6 GHz: 0.99 | 0.11; 6-12 GHz: 1.39 | 0.65)) (Accuracy in RMSE)	0.5 – 12	L	Water, TX-100	[91]
Breast (Fat, Malignant Tissue, Skin) (Not imitating actual tissues but their contrast)	1 – 11	L	Water, Oil, Diacetin, FR4 Glass Epoxy Printed Circuit Board (PCB)	[92]
Blood (1.25 | 0.09), **Cartilage** (0.38 | 0.45), **Colon** (0.22 | 0.26), **Colon Malignant** (0.45 | 1.05), **Cornea** (1.44 | 0.84), **Grey Matter** (1.74 | 0.58), **Heart** (0.47 | 0.7), **Kidney** (0.99 | 0.18), **Liver** (0.38 | 0.29), **Muscle** (0.43 | 0.47), **Pancreas** (0.54 | 0.69), **Wet Skin** (0.53 | 0.32) (Accuracy in RMSE*)	0.5 – 18	L	Water, Acetonitrile, Ethanol, Sodium Chloride	[39], [41], [93]
Infiltrated Fat, **Non-Infiltrated Fat**, **Muscle**, **Wet Skin**, **Dry Skin** (Accuracy not provided)	0.5 – 20	SS	Water, Gelatine, Oil, Formaldehyde, Surfactant, n-Propanol, p-Toluic Acid	[94]
2/3 Muscle (Accuracy not provided)	2 – 10	SS	Water, Agar, Polyethylene Powder, Sodium Chloride, TX-151, Dehydroacetic Acid Sodium Salt	[95]
Breast (Fat (9%), Gland (14%), Tumor (9%)) (Accuracy in deviation for real part)	3.1 – 10.6	SS	Water, Gelatine, Oil, Propylene Glycol, Surfactant, Formaldehyde, Agar, p-Toluic Acid, 1-Propanol, Alizarin	[96]
Breast (Low Density (2 types, 1.22/2.59 | 2.39/3.19), High Density (2.89 | 2.17)) (Accuracy in RMSE at 7.5 GHz)	3 – 11	SS	Water, Propylene Glycol, Gelatine, Oil, Surfactant, Glyoxal, Glutaraldehyde, Agar, Cornflour	[97]
Wet Skin (6.87 | 5.97 S^2/m^2), **Fat** (0.21 | 0.29 S^2/m^2), **Blood** (25.38 | 1.12 S^2/m^2), **Muscle** (21.14 | 6.21 S^2/m^2) (Accuracy in MSE)	0.3 – 20	SS	Water, Oil, Gelatine, Sodium Chloride, Detergent	[98]
Breast (Muscle, Fibrograndular Tissue, Skin, Transitional Tissue, Fat, Malignant Tissue) (Accuracy not provided)	3 – 10	SS	Water, Glycerin, Polyethylene Powder, Agar	[99]
Breast (Fat, Tumor, Skin) (Not imitating actual tissues but their contrast)	2 – 12	SS	Water, Wheat Flour, Petroleum Jelly (Vaseline), Oil, Glass	[100]
Fat, **Muscle**, **Grey Matter** (First order match)	0.001 – 10	S	Carbon Black Powder, PTFE Powder	[101]
Breast (Normal, Tumor) (Accuracy not provided)	2 – 10	S	Polycarbonate, Oil, Epoxy	[102]
Skin (2 types, 28/10 | 21/31), **Bone** (7 | 47), **Fat** (2.46 | 0.15 S/m) (Accuracy in relative error in 2-10 GHz except absolute error for fat)	1 – 10	S	Carbon Black Powder, Graphite Powder, Silicone Rubber, Urethane Rubber	[103]
Liver (3 models, 8.58/8.55/7.77 | 5.49/5.77/6.47) (Accuracy in RMSE+)	0.7 – 20	S	Water, Sucrose, Sodium Chloride, HEC 4400, Dowicil 75	[104]
Breast (Muscle, Fat, Dry and Wet Skin, Malignant Tissue) (Accuracy not provided)	2 – 15	V	Water, Slime, Egg White, Egg Yolk, Butter, Glycerol, Moisturing Lotion, Cornstarch	[105]

* Own measurements after preparing and measuring the phantoms within 3.1 – 10.6 GHz
+ Calculation using the parametric models provided in the study within 3.1 – 10.6 GHz
L: Liquid, SS: Semisolid, S: Solid, V: Various

on the application, these phantoms can be solid [106], semisolid [107] or liquid [108]. Concretely, the emulation of an in-body communications scenario usually requires a liquid where the implanted antenna can be freely placed and moved. Moreover, the physical properties of phantoms also restrict the materials used, and thus the values of relative permittivity that can be achieved. For instance, liquid phantoms are frequently composed of a high amount of water, which is suitable to mimic soft tissues; whereas solids use polymers whose dielectric constant is lower. Apart from the dielectric features, other attributes like non-hazard, low-cost, easy-to-prepare and long lifespan are desired. As target data to imitate, there are three possibilities. Firstly, selecting measured data of real tissues from previous authors. In that case, most works use Gabriel's reference [30], or recent works based on it [109], in which parametric models are provided for many tissues. Secondly, others perform their own measurements according to their requirements [110]. Finally, some researchers estimate theoretically the relative permittivity, taking into account the tissue constituents [111].

In the literature, formulas for phantom preparation are given for a specific frequency range [112]. In particular, some researchers model broadband phantoms [94], [107], [110], covering a specific frequency range. Table II reviews of those phantoms reported in the literature that include the UWB frequency band. Ingredients vary from basic compounds [40], [105] to laboratory chemicals [94], [96]. As can be seen, certain compounds such as water, sodium chloride, oil and flour are common in several references. These compounds constitute the main influence on the relative permittivity among others like polymer powders or polar liquids. The rest of the constituents attempt to provide some desired physical properties. For example, gelatine and agar are used to get semisolid phantoms, surfactants permit mixing insoluble compounds and alizarin is used as a colorant.

The accuracy of phantoms with respect to real tissues is often specified by the root-mean-square error (RMSE), but also by the mean squared error (MSE) and the relative error. From Table II, one can observe that many of them have large deviations [40], [96], [98], [101], [103], [104]. Others do not even conform to tissue values, but such phantoms are created so that the differences between their values are equivalent to those of the tissues of interest [92], [100]. Inasmuch as breast phantoms are one of the most pursued, they attain a good accuracy in some works [91], [97]. Muscle phantoms, in particular, are given in four different works in Table II, with a high contrast between their errors. Both [40] and [98] exhibit a high deviation from the reference values, whereas [101] just provides a first-order match. The muscle phantom from [39], [41] has the highest accuracy, with a really low RMSE. Regarding skin phantoms, the best-case error for the dielectric constant is 21% [103]. The values for wet skin are provided in a wider frequency range in [41] and [98], however, the broadest band is achieved at the expense of accuracy. Certainly, imitating the relative permittivity of tissues in such a large bandwidth is challenging. The dielectric values must be fitted to those of body tissues as well as their trend with frequency. Dipole relaxation frequency is the key factor when a wideband phantom is sought, since it defines how the relative permittivity changes with frequency. This parameter is especially crucial in tissues with high water content, owing to the fact that their dielectric properties are more frequency-dependent than tissues with low water content. This behavior explains why low water-content tissues are normally obtained with great accuracy, e.g., the fat [94], [98], [103]. Acetonitrile aqueous solutions have been recently suggested to replicate the curve behavior of tissues within the microwave frequency bands [39], [41], [93]. Besides, a fine adjustment to the target values can be achieved by adding some extra compounds, so that a phantom can be tailored to different tissues.

The list of mimicked tissues still needs to be enlarged, so that one can assemble a realistic heterogeneous model. As previously mentioned, many phantoms are designed for microwave imaging for breast cancer detection [91], [92], [96], [97], [99], [100], [102], [105]. In contrast, formulas for gastrointestinal phantoms are less studied [40], [41], [94], [104], restricting the possibilities to accurately testing those in-body devices which could make use of the UWB benefits to improve their performance, e.g. capsule endoscope. As an example, a liquid phantom made of water with sucrose has been proposed with the aim of performing propagation studies in the UWB band [40]. Some authors use this approach to carry out in-body propagation experiments [16], since it is a simple mixture which can be easily prepared in laboratory facilities. Nevertheless, this phantom only mimics the muscle, and its dielectric properties are rather far from the actual ones. Another work suggests an average human-torso phantom using a 2/3 muscle equivalent [95]. However, since it is not a multilayer phantom, reflections inside the medium cannot be comparable to a real body. This deficiency might be overcome

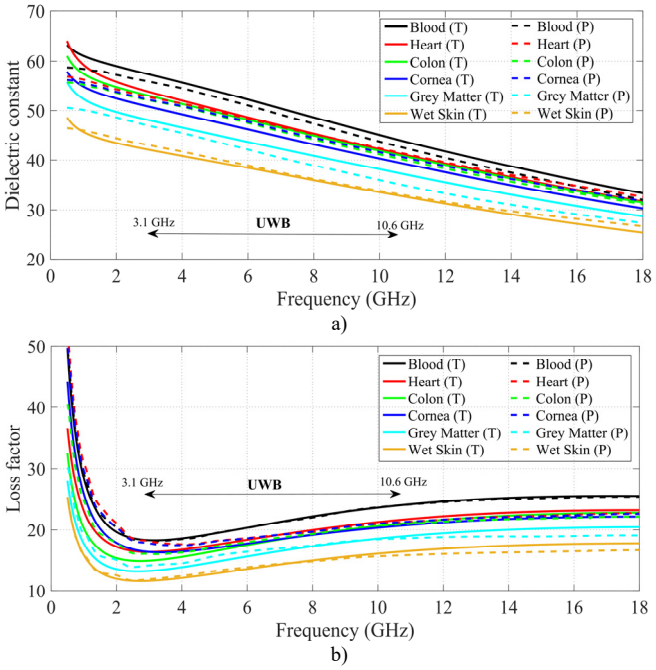

Fig. 5. Relative permittivity of several phantoms [39], [41] (dashed lines) in comparison with the real values [30] of their corresponding tissues (solid lines). a) Dielectric constant b) Loss factor.

by the synthetic model patented in [41] since it provides several mimicked tissues specially designed for the UWB frequency band. Indeed, authors fit the reference values within a larger frequency band, as can be observed in Fig. 5. Their values for six tissue types are compared to Gabriel's data [30]. Thus, this model improves the accuracy of all the others depicted in Table II and provides phantoms for tissues which have not been suggested before in such wide bands. This advancement could lead to realistic models by combining phantoms of different tissues in a multi-layered way. Furthermore, this synthetic model may be used for making different sorts of studies, such as specific absorption rate (SAR) [113], microwave imaging [114], radiation dosimetry studies [115] or propagation through human body [116].

III. Propagation through Human Tissues

The location of the nodes involved in the communication among wireless sensors establishes the propagation scenario. For in-body propagation three different scenarios can be considered when at least one of the nodes is implanted inside the body [13]:

- In-Body to In-Body (IB2IB) scenario, where all nodes involved in the communication are located inside the human body.
- In-Body to On-Body (IB2OB) scenario, where the implanted sensors communicate with nodes located in direct contact with the human body surface.
- In-Body to Off-Body (IB2OFF) scenario, where the in-body sensors communicate with an external node located far away from the body surface.

In these three scenarios, the sensor implanted inside the body typically acts as a transmitter whereas on-body or off-body nodes act as receivers. One example is the wireless capsule endoscopy [117], which captures images during its travel along the gastrointestinal tract propelled by peristaltic movements [118]. Then, the images are sent through the human body tissues to an on-body sensor array located on the waist. Another example is the peacemaker which incorporates small sensors to monitor vital signs [119]. The collected information is also sent from inside the thoracic cavity to outside the human body wirelessly.

A. Antennas for UWB In-body Communications

As can be easily predicted, both in-body and external antennas play an essential role in establishing a proper link among the nodes. As detailed in the previous section, the relative permittivity of human tissues varies according to the selected working radio frequency [30]. Moreover, the behavior and performance of WBAN in-body antennas can be affected by the surrounding medium [32]. Hence, the inclusion of human tissues in the design stage of these kinds of antennas is highly relevant. Since implanted antennas are completely wrapped by human tissues, designers of such kind of antennas mainly seek two characteristics On the one hand, in-body antennas should have an omnidirectional radiation pattern in order to communicate with a sensor array located outside the body, e.g. around the human waist [120], [121]. The use of this radiation pattern instead of a directional one can minimize the possibility of not receiving any radio signal from certain locations inside the body since it moves uncontrollably [122]. On the other hand, the antenna matching should be ensured within the entire frequency range of interest. In [123], the authors focused on designing a suitable tiny UWB antenna to be implanted inside the brain, whereas in [124] experts designed and manufactured a UWB antenna, which works in the low part of UWB spectrum, to be embedded in the capsule endoscope. Most implantable antennas are miniaturized and optimized to work in high frequencies in the first designing stage [124], [125]. After that, in-body antennas are wrapped with human tissue layers. Subsequently, we can expect that the resonance frequency shifts down due to the dielectric properties of human tissues and thus an antenna matching within the bandwidth of interest is obtained [32]. This optimization and miniaturization procedure may not be efficient for antenna designs which work with a large bandwidth. This is due to the fact that human tissues are frequency dependent and consequently the antenna can be affected in different manners at different frequencies. Moreover, the high losses in this propagation medium can also irreversibly vary the free-space radiation parameters. In order to characterize the available radio channel performance provided by UWB, new optimization and miniaturization techniques should be used to obtain reliable antenna candidates. The use of direct optimization procedures at the initial antenna designing stage [126] profits from the human tissue properties for antenna miniaturization.

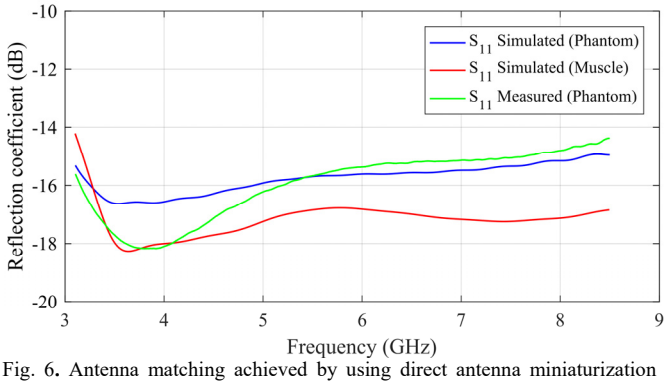

Fig. 6. Antenna matching achieved by using direct antenna miniaturization procedure [127].

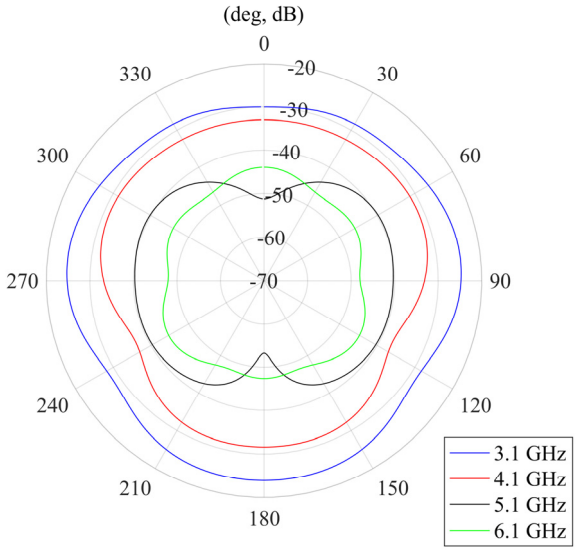

Fig. 7. Radiation pattern of an implanted antenna at UWB frequencies by using antenna miniaturization procedure [127].

Thus, the targets of radiation parameters (see Fig. 6 and Fig. 7) can be easily accomplished.

Moreover, on-body receiving antennas for IB2OB scenarios must achieve an antenna matching when they are located between layers of human tissues in front and air at the rear [128]. Furthermore, wave propagation conditions through body tissues should be achieved. In addition, the use of a beam antenna rather than an omnidirectional one is preferable for this purpose. This fact can mitigate the reception of unwanted interfering signals as well as focusing usefully the power towards the human body increasing the antenna gain. In the literature, a large number of UWB on-body antenna designs for on-body to on-body and on-body to off-body communications can be found [129]–[131]. Some UWB on-body antenna designs such as helix antennas [132] or slotted-patch antennas [133] have been assessed to communicate with implants. However, more research studies to design new UWB on-body receivers should be encouraged to validate UWB for future in-body networks.

TABLE III
REPORTED PATH LOSS MODELS IN THE UWB BAND

Scenario	Methodology of Analysis	Frequency Range (GHz)	Distance Range (cm)	Scenario of Application	Path Loss Model	Reference
IB2IB	Experimental Measurements	3.1 – 8.5	$3 \le d \le 8$	Muscle Tissue	Linear*	[134]
IB2OB	Numerical Simulations	1 – 6	$1 \le d \le 15$	Abdominal Region	Linear*	[135]
			$0.1 \le d \le 12$	Chest Region	Power*	[136]
		3.1 – 6	$4 \le d \le 6$	Chest Region	Log-distance*+	[137]
		3.4 – 4.8	$5 \le d \le 9$	Abdominal Region	Log-distance	[138]
			$2 \le d \le 24$		Log-distance*	[139]
	Numerical simulations & Experimental measurements	3.5 – 4.5	$0 \le d \le 9$	Abdominal Region	Power*	[140]
	Experimental Measurements	3.1 – 8.5	$5.5 \le d \le 20$	Muscle Tissue	Log-distance*	[134]
	Experimental & *In vivo* measurements	3.1 – 5	$3 \le d \le 11$	Muscle Tissue/ Abdominal Region	Linear	[31]
	In vivo measurements	1 – 6	$5 \le d \le 16$	Abdominal Region	Log-distance	[43]
		3.4 – 4.8	$3 \le d \le 12$	Abdominal Region	Log-distance*	[44]

* Adding a shadowing term
\+ Depending on frequency

B. *UWB Radio Channel Performance*

With the aim of enhancing the current standard 802.15.6-2012 for in-body communications by using the UWB spectrum, more reliable radio link analysis should be performed to consider UWB frequency range as the best candidate for this purpose. In the literature, a large amount of studies focused on UWB implant channel characterization using different methodologies are reported. They are summarized in Table III.

As explained in the introduction section, there are three approaches to study the in-body propagation channel:

- *Simulations by means of electromagnetic software*. As mentioned before, the features of radio channel are investigated by using well-known computer software such as CST® [136] or HFSS™ [141]. Complex heterogeneous multilayer structures can be obtained by using anatomical models of human tissues [33].
- *Experimentally*, by means of channel measurements using a VNA which measures the S_{21} parameter as shown in Fig. 8. Those measurements can be divided into two categories:
  - *Laboratory tests. Use of tissue-mimicking phantoms*. Materials which emulate the dielectric properties of human tissues can be a really cost-effective way to reproduce the implant radio channel feasibly [41], [110].
  - *In vivo measurements –animal experimentation–*. Since human experimentation is highly restricted, the use of animal subjects is a feasible option in order to get the real propagation conditions when radio waves go through different living tissues [42], [43].

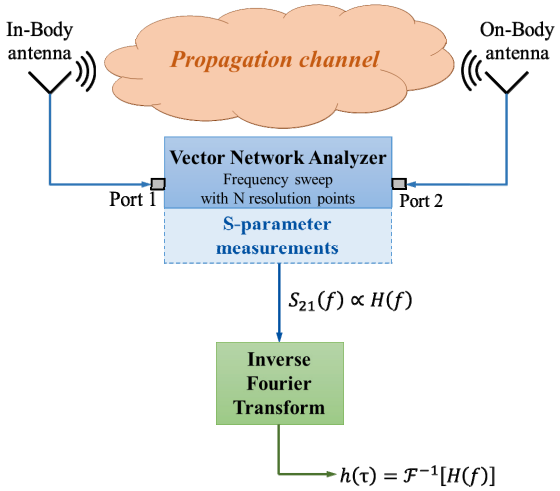

Fig. 8. Experimental channel sounding of the IB2OB channel by using a VNA.

Regardless of the methodology of analysis, the main radio channel feature reported in the literature is the path loss and its fitting model. Thus, the path loss models found in the literature can be classified depending by their dependence on distance as:

- *Linear*, in which the path loss in decibels varies linearly (slope α) with the distance between antennas, d, as: $PL(dB) = C + \alpha d$ where is C a constant.
- *Power*, where the path loss in decibels varies with the power (exponent γ) of the distance between antennas as: $PL(dB) = C + \alpha d^{\gamma}$.
- *Log-distance*, in which the path loss in decibels is linearly dependent (slope n) with the logarithm of the distance between antennas as: $PL(dB) = C + 10n\log(d)$.

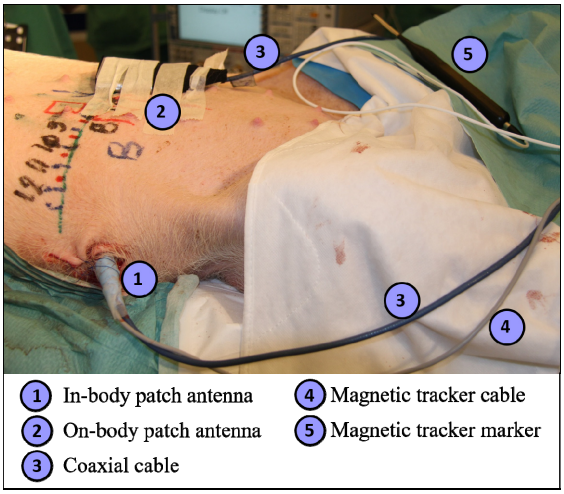

Fig. 9. *In vivo* measurement setup [31].

Sometimes, those models also include a shadowing term that statistically models –typically with a Gaussian function– the dispersion of the samples around the fitting model. However, the models available in the literature vary considerably depending on the scenario, the range of the distance between antennas considered, and the frequency band analyzed as detailed in Table III and explained in the following.

The real propagation conditions of body tissues can be reproduced by using living animals (see Fig. 9) such as pigs, since the electromagnetic properties of their tissues are quite similar to those of human at microwave frequencies [140]. The behavior of losses within a specific distance range between sensors can vary according to the tissues involved in the communication, the used bandwidth, etc. In [31] and [44], engineers and medical specialists performed an IB2OB measurement campaign by using a pig subject. The used bandwidth is quite similar in both works as well as the distance between transmitters and receivers (3.1-5 GHz from 3 to 11 cm and 3.1-4.8 GHz from 3 to 12 cm, respectively). Nonetheless, the path loss is well-fitted by a log-distance model in [31] whereas the best fit is achieved by a linear approximation model in [44]. These discrepancies between the path loss approximation models can be produced due to the fact that pig subjects chosen for each *in vivo* experiment as well as the transmitting and receiving antennas are different. Furthermore, the received power is highly influenced by the tissues that radio waves go through, i.e., the tissues of the thoracic cavity are not the same as those of the abdominal region. Besides, a large amount of measurement points should be taken in each experimental campaign to validate the model. Authors in [43] extend the bandwidth from 1 to 6 GHz as well as the distance between antennas from 5 to 16 cm in an IB2OB scenario using a pig as well. In this case, the path loss is well-fitted again by a log-distance model but the number of measurement points is still low.

Although the use of living animals seems to be the most reliable way to study the in-body radio channel characteristics, animal experimentation is highly restricted due to ethical reasons. Besides, the necessity of a conditioned operating room as well as medical instruments could raise the charges considerably. Thus, research studies focused on validating the UWB frequency range as a candidate for future implant devices use other cost-effective ways such as electromagnetic computation software or experimental phantoms for laboratory tests. With regard to computer simulators, the most popular measurements use sophisticated anatomical models such as Hugo and Nelly from Visible Human Project, or the Virtual Population designed by ITIS foundation (see Table I). In this manner, one can emulate the transmission through the different body tissues within countless positions of involved nodes. In [136], authors approximated the losses by means of a numerical statistical model (see Table III) from 0.1 to 12 cm within a frequency band from 1 to 6 GHz. In this study, implanted probes are located within a rectangular volume close to the heart whereas an incoming plane wave is transmitted from outside the body to the human chest. However, most research works are focused on the propagation around the human abdominal region, e.g., recreating the typical scenario in which a capsule endoscope sends images to an on-body sensor array located on the waist. Accordingly, authors proposed in [135] a path loss approximation model for the abdominal region which is quite similar to that obtained in [136] for the thoracic cavity within the same frequency range and similar depth from the skin. The changes between path loss models may be produced by the different tissues involved in each scenario. Other studies only consider frequency bands within the UWB frequency range as proposed [138]–[140]. Even though both the distance range and the frequency bandwidth vary among works, the losses follow a logarithmic trend.

As mentioned above, the use of experimental phantoms could be a reliable, and effective solution to emulate the electromagnetic behavior of human tissues in laboratory tests that can be carried out easily. Nevertheless, the UWB radio channel characterization by using liquid phantoms is challenging. As outlined in Section II.B, achieving highly accurate phantoms in a large bandwidth for different body tissues can be an unrealizable task. Furthermore, transmitters and receivers involved in the propagation scenario should be moved accurately to different locations in order to research the radio channel characteristics, knowing the position of the sensors as well as the distance between antenna centers. In [134], authors performed a measurement campaign within UWB (3.1-8.5 GHz) by using a novel experimental setup (see Fig. 10).

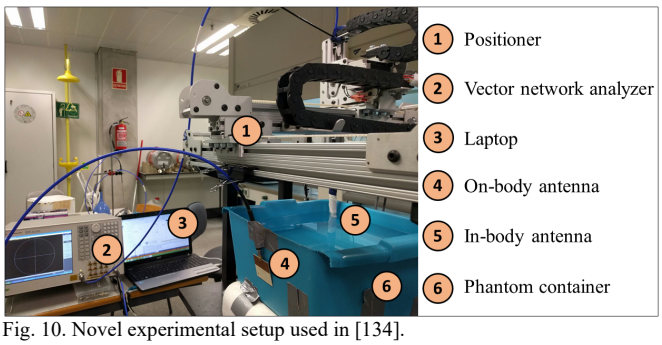

Fig. 10. Novel experimental setup used in [134].

Authors used a high accurate muscle phantom reported in [39], [41], which achieves the best approximation of the relative permittivity of human muscle tissue within UWB (see Table II). Two common scenarios were reproduced by means of this setup (IB2OB and IB2IB). On the one hand, authors conclude that the path loss approximation model which best fits the losses is the linear model for the IB2IB scenario and the shadowing is well-fitted by a normal distribution from 3 to 8 cm. The trend of the losses matches the results obtained in other studies within other frequency ranges [16]. It is hard to find research works devoted to UWB IB2IB scenarios in order to perform a thorough comparative of path loss models. Therefore, more studies to enhance the communication among implanted sensor networks should be conducted. On the other hand, the path loss is fitted by a log-distance model for the IB2OB scenario, as concluded in [134]. Likewise, the shadowing is well-fitted by a normal distribution. This path loss model is quite similar to those obtained by using computer heterogeneous human models [136], other phantom-based setups [140] and those computed from *in vivo* measurements [31] within the same distance range between antenna centers.

As illustrated in Fig. 11, reaching a common path loss model for all the aforementioned cases is challenging. As already pointed out, the tissues involved in the propagation scenario can affect the trend of the path loss model as noted by comparing [31] and [44]. Moreover, the considered scenario as well as the involved tissues determine the performance of the radio link. Besides, the transmitting and receiving antennas play an important role for the characterization of the in-body radio channel characterization. The chosen bandwidth within UWB can determine the most suitable approximation model, so the frequency dependence of the UWB in-body radio channel characteristics should be considered. Despite these discrepancies, the path loss model which exhibits the best fit for the IB2IB scenario within UWB is the linear approximation model, whereas the log-distance is the most suitable one for the IB2OB scenario. The literature lacks of research works within UWB for in-body applications, thus many more studies should be performed to achieve a standardized path loss model.

C. Correlation

Channel diversity of UWB systems can enhance the channel performance and thus enable new applications. UWB systems can achieve highly accurate localization algorithms [142] and multiantenna systems. These techniques can be influenced by the correlation among transmitters and receivers [143]. Hence, future algorithms for the localization of implanted sensors, such as the capsule endoscope, may be affected by the channel diversity in both transmission and reception.

Regarding the correlation in transmission -calculated to study the diversity of the UWB in-body channel in several locations of transmitting antennas- it decreases rapidly whatever the distance between transmitter antennas was, as authors concluded in [134], in an IB2IB phantom-based setup.

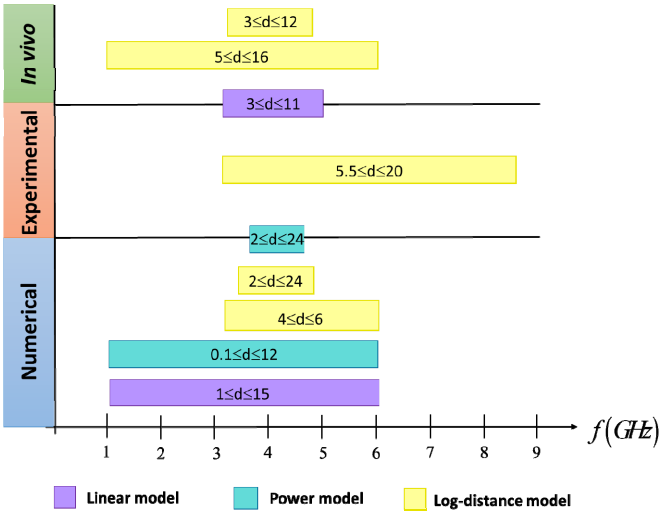

Fig. 11. Chart of the UWB path loss models proposed in the literature for IB2OB scenario for different frequency bands and range distances (expressed in centimeters).

They also concluded that correlation is quite high when transmitting antennas are aligned at the same height and the distance between their centers is below 5 cm for the IB2OB scenario. Other techniques such as designing new dual-polarized implantable transmitters could help to increase the diversity of the channel in transmission [44].

The diversity in reception is assessed by considering different receiving antenna locations. In [134], the study concluded that correlation decreases as the distance between the receiving antennas increases, as in [144]. Besides, the receiving antennas should be separated more than one wavelength in order to increase the diversity in reception, i.e., to obtain uncorrelated signals in reception.

However, few studies deal with UWB in-body channel diversity, unlike the body of works for off-body scenarios [145]. Therefore, further research works should aim at performing thorough studies focused on this area. In this manner, new medical applications based on UWB can be pre-evaluated to strengthen the candidature of this technology for this purpose.

IV. Conclusions and Perspectives

UWB propagation for in-body sensor networks can be considered as a complex environment where the antennas, the propagation medium and the methodology of analysis impact the overall behavior of the in-body radio channel. Many research works about UWB in-body propagation can be found in the literature. However, results are hard to compare due to the differences in these key factors involved. Therefore, a general channel model has not been reported yet so that standardization for future in-body UWB devices can become difficult.

In this work, the authors have reviewed the current state of the art for the UWB in-body propagation environment by addressing: the characteristics of the propagation medium, i.e., the human body tissues; the role of the in-body antennas; and the key aspects of every analysis method (software

simulations, phantom-based measurements and *in vivo* measurements). Thus, the main outcomes of this work are:

1) The dielectric properties of human body tissues and their frequency dependency impact considerably both the theoretical and the experimental analysis of the in-body radio channel.
2) Mathematical simulations of the UWB in-body propagation channel imply the need for accurate computer human models.
3) Phantoms for experimental analysis within UWB should comply with the dielectric values of the different body tissues as well as their trend in such a large frequency band.
4) In-body and on-body antennas should be designed taking into account the propagation medium. The antennas should be designed considering the surrounding tissue from the very initial stages of the designing process.
5) Most propagation studies for in-body communications in UWB, model the in-body radio channel as a log-distance model. However, the in-body radio channel is very influenced by a) the methodology of analysis (theoretical simulations or experimental measurements), b) the antennas used as well as their performance, and c) the channel behavior and the scenario considered (abdominal region, chest, etc.). Therefore, an in-depth study is necessary in order to develop a general model, whatever the scenario under analysis.

Future trends in research on in-body propagation within UWB band should try to overcome these challenges. Firstly, a multilayer accurate UWB phantom for in-body measurements is necessary in order to carry out extensive and realistic measurement campaigns. Furthermore, the design of more efficient antennas, that can counter the high losses of body tissues at UWB, would play a key role in a future use of the UWB band for medical devices. Finally, not only a path loss model but also a delay domain model of the in-body radio channel should be addressed in the literature. This complete model would be of utmost importance for further algorithms based on radio information such as location of in-body devices or interferences among several devices implanted inside the human body.

REFERENCES

[1] E. Jovanov and A. Milenkovic, "Body Area Networks for Ubiquitous Healthcare Applications: Opportunities and Challenges," *J. Med. Syst.*, vol. 35, no. 5, pp. 1245–1254, Oct. 2011.

[2] M. Patel and J. Wang, "Applications, challenges, and prospective in emerging body area networking technologies," *IEEE Wirel. Commun.*, vol. 17, no. 1, pp. 80–88, Feb. 2010.

[3] E. Y. Chow, A. L. Chlebowski, and P. P. Irazoqui, "A Miniature-Implantable RF-Wireless Active Glaucoma Intraocular Pressure Monitor," *IEEE Trans. Biomed. Circuits Syst.*, vol. 4, no. 6, pp. 340–349, Dec. 2010.

[4] M. Waqialla, R. Alshammari, and M. I. Razzak, "An ontology for remote monitoring of cardiac implantable electronic devices," in *2015 International Conference on Computer, Communications, and Control Technology (I4CT)*, Kuching, 2015, pp. 520–523.

[5] A. Stango, K. Y. Yazdandoost, F. Negro, and D. Farina, "Characterization of In-Body to On-Body Wireless Radio Frequency Link for Upper Limb Prostheses," *PLoS One*, vol. 11, no. 10, pp. 1–19, Oct. 2016.

[6] G. Pan and L. Wang, "Swallowable Wireless Capsule Endoscopy: Progress and Technical Challenges," *Gastroenterol. Res. Pract.*, vol. 2012, pp. 1–9, 2012.

[7] K. Y. Yazdandoost and R. Miura, "SAR studies for UWB implanted antenna for Brain-Machine-Interface application," in *2016 10th European Conference on Antennas and Propagation (EuCAP)*, Davos, 2016, pp. 1–4.

[8] B. Ciftcioglu *et al.*, "3-D integrated heterogeneous intra-chip free-space optical interconnect," *Opt. Express*, vol. 20, no. 4, pp. 4331–4345, Feb. 2012.

[9] G. E. Santagati and T. Melodia, "Sonar inside your body: Prototyping ultrasonic intra-body sensor networks," in *IEEE INFOCOM 2014 - IEEE Conference on Computer Communications*, Toronto, ON, 2014, pp. 2679–2687.

[10] R. Cavallari, F. Martelli, R. Rosini, C. Buratti, and R. Verdone, "A Survey on Wireless Body Area Networks: Technologies and Design Challenges," *IEEE Commun. Surv. Tutorials*, vol. 16, no. 3, pp. 1635–1657, 2014.

[11] B. Gulbahar, "Theoretical Analysis of Magneto-Inductive THz Wireless Communications and Power Transfer With Multi-Layer Graphene Nano-Coils," *IEEE Trans. Mol. Biol. Multi-Scale Commun.*, vol. 3, no. 1, pp. 60–70, Mar. 2017.

[12] IEEE Standards Association, *802.15.6-2012 - IEEE Standard for Local and metropolitan area networks - Part 15.6: Wireless Body Area Networks*. Institute of Electrical and Electronics Engineers, 2012.

[13] R. Chávez-Santiago *et al.*, "Propagation models for IEEE 802.15.6 standardization of implant communication in body area networks," *IEEE Commun. Mag.*, vol. 51, no. 8, pp. 80–87, Aug. 2013.

[14] K. Sayrafian-Pour, W.-B. Yang, J. Hagedorn, J. Terrill, K. Yekeh Yazdandoost, and K. Hamaguchi, "Channel Models for Medical Implant Communication," *Int. J. Wirel. Inf. Networks*, vol. 17, no. 3–4, pp. 105–112, Dec. 2010.

[15] K. Sayrafian-Pour, W.-B. Yang, J. Hagedorn, J. Terrill, and K. Y. Yazdandoost, "A statistical path loss model for medical implant communication channels," in *2009 IEEE 20th International Symposium on Personal, Indoor and Mobile Radio Communications*, Tokyo, 2009, pp. 2995–2999.

[16] R. Chavez-Santiago *et al.*, "Experimental Path Loss Models for In-Body Communications within 2.36-2.5 GHz.," *IEEE J. Biomed. Heal. informatics*, vol. 19, no. 3, pp. 930–937, Apr. 2015.

[17] D. Kurup *et al.*, "In-body path loss models for implants in heterogeneous human tissues using implantable slot dipole conformal flexible antennas," *EURASIP J. Wirel. Commun. Netw.*, vol. 2011, no. 51, pp. 1–9, Dec. 2011.

[18] D. Kurup, W. Joseph, G. Vermeeren, and L. Martens, "In-body path loss model for homogeneous human tissues," *IEEE Trans. Electromagn. Compat.*, vol. 54, no. 3, pp. 556–564, Jun. 2012.

[19] S. Ashok Kumar and T. Shanmuganantham, "Design and Analysis of an Implantable CPW-Fed X-Monopole Antenna for 2.45-GHz ISM Band Applications," *Int. J. Microw. Wirel. Technol.*, vol. 20, no. 3, pp. 246–252, Mar. 2014.

[20] J. Gemio, J. Parron, and J. Soler, "Human body effects on implantable antennas for ISM bands applications: models comparison and propagation losses study," *Prog. Electromagn. Res.*, vol. 110, pp. 437–452, 2010.

[21] R. de Francisco and A. Pandharipande, "Spectrum occupancy in the 2.36–2.4 GHZ band: Measurements and analysis," in *2010 European Wireless Conference (EW)*, Lucca, 2010, pp. 231–237.

[22] P. Patel, M. Sarkar, and S. Nagaraj, "Ultra wideband channel characterization for invasive biomedical applications," in *2016 IEEE 17th Annual Wireless and Microwave Technology Conference (WAMICON)*, Clearwater, FL, 2016, pp. 1–6.

[23] A. F. Molisch, "Ultra-Wide-Band Propagation Channels," *Proc. IEEE*, vol. 97, no. 2, pp. 353–371, Feb. 2009.

[24] A. Ghildiyal, K. Amara, R. D. Molin, B. Godara, A. Amara, and R. K. Shevgaonkar, "UWB for in-body medical implants: A viable option," in *2010 IEEE International Conference on Ultra-Wideband*, Nanjing, 2010, pp. 1–4.

[25] R. Chávez-Santiago, I. Balasingham, and J. Bergsland, "Ultrawideband Technology in Medicine: A Survey," *J. Electr. Comput. Eng.*, vol. 2012, pp. 1–9, 2012.

[26] E. Y. Chow, M. M. Morris, and P. P. Irazoqui, "Implantable RF Medical Devices: The Benefits of High-Speed Communication and Much Greater Communication Distances in Biomedical Applications," *IEEE Microw. Mag.*, vol. 14, no. 4, pp. 64–73, Jun. 2013.

[27] R. Chávez-Santiago and I. Balasingham, "Ultrawideband Signals in Medicine [Life Sciences]," *IEEE Signal Process. Mag.*, vol. 31, no. 6, pp. 130–136, Nov. 2014.

[28] M. R. Yuce and T. Dissanayake, "Easy-to-Swallow Wireless Telemetry," *IEEE Microw. Mag.*, vol. 13, no. 6, pp. 90–101, Sep. 2012.

[29] A. Khaleghi, R. Chávez-Santiago, and I. Balasingham, "An improved ultra wideband channel model including the frequency-dependent attenuation for in-body communications," in *Proceedings of the Annual International Conference of the IEEE Engineering in Medicine and Biology Society, EMBS*, San Diego, CA, 2012, pp. 1631–1634.

[30] C. Gabriel, "Compilation of the Dielectric Properties of Body Tissues at RF and Microwave Frequencies," Occupational and environmental health directorate, Radiofrequency Radiation Division, Brooks Air Force Base, Texas (USA), Jun. 1996.

[31] C. Garcia-Pardo *et al.*, "Experimental ultra wideband path loss models for implant communications," in *2016 IEEE 27th Annual International Symposium on Personal, Indoor, and Mobile Radio Communications (PIMRC)*, Valencia, 2016, pp. 1–6.

[32] P. S. Hall and Y. Hao, *Antennas and propagation for body-centric wireless communications*. Norwood, MA: Artech House, 2012.

[33] A. Christ *et al.*, "The Virtual Family—development of surface-based anatomical models of two adults and two children for dosimetric simulations," *Phys. Med. Biol.*, vol. 55, no. 2, pp. N23–N38, Jan. 2010.

[34] V. M. Spitzer and D. G. Whitlock, "The visible human dataset: The anatomical platform for human simulation," *Anat. Rec.*, vol. 253, no. 2, pp. 49–57, Apr. 1998.

[35] H. B. Lim, D. Baumann, and E.-P. Li, "A Human Body Model for Efficient Numerical Characterization of UWB Signal Propagation in Wireless Body Area Networks," *IEEE Trans. Biomed. Eng.*, vol. 58, no. 3, pp. 689–697, Mar. 2011.

[36] R. Chávez-Santiago *et al.*, "Experimental implant communication of high data rate video using an ultra wideband radio link," in *2013 35th Annual International Conference of the IEEE Engineering in Medicine and Biology Society (EMBC)*, Osaka, 2013, pp. 5175–5178.

[37] R. Chávez-Santiago, C. Garcia-Pardo, A. Fornes-Leal, A. Vallés-Lluch, I. Balasingham, and N. Cardona, "Ultra wideband propagation for future in-body sensor networks," in *2014 IEEE 25th Annual International Symposium on Personal, Indoor, and Mobile Radio Communication (PIMRC)*, Washington, DC, 2014, pp. 2160–2163.

[38] T. Takimoto, T. Onishi, K. Saito, M. Takahashi, S. Uebayashi, and K. Ito, "Characteristics of biological tissue equivalent phantoms applied to UWB communications," *Electron. Commun. Japan, Part I Commun. (English Transl. Denshi Tsushin Gakkai Ronbunshi)*, vol. 90, no. 5, pp. 48–55, May 2007.

[39] S. Castelló-Palacios, C. Garcia-Pardo, A. Fornes-Leal, N. Cardona, and A. Vallés-Lluch, "Tailor-Made Tissue Phantoms Based on Acetonitrile Solutions for Microwave Applications up to 18 GHz," *IEEE Trans. Microw. Theory Techn.*, vol. 64, no. 11, pp. 3987–3994, Nov. 2016.

[40] H. Yamamoto, J. Zhou, and T. Kobayashi, "Ultra wideband electromagnetic phantoms for antennas and propagation studies," *IEICE Trans. Fundam. Electron. Commun. Comput. Sci.*, vol. E91–A, no. 11, pp. 3173–3182, Nov. 2008.

[41] N. Cardona, S. Castelló-Palacios, A. Fornes-Leal, C. Garcia-Pardo, and A. Vallés Lluch, "Synthetic Model of Biological Tissues for Evaluating the Wireless Transmission of Electromagnetic Waves," Patent WO/2017/109252, 30-Jun-2017.

[42] D. Anzai *et al.*, "Experimental Evaluation of Implant UWB-IR Transmission With Living Animal for Body Area Networks," *IEEE Trans. Microw. Theory Techn.*, vol. 62, no. 1, pp. 183–192, Jan. 2014.

[43] P. A. Floor *et al.*, "In-Body to On-Body Ultrawideband Propagation Model Derived From Measurements in Living Animals," *IEEE J. Biomed. Heal. Informatics*, vol. 19, no. 3, pp. 938–948, May 2015.

[44] Y. Shimizu, D. Anzai, R. Chavez-Santiago, P. A. Floor, I. Balasingham, and J. Wang, "Performance Evaluation of an Ultra-Wideband Transmit Diversity in a Living Animal Experiment," *IEEE Trans. Microw. Theory Techn.*, vol. 65, no. 7, pp. 2596–2606, Jul. 2017.

[45] J. D. Taylor, *Ultrawideband Radar: Applications and Design*. CRC Press, 2012.

[46] C. Li, M.-R. Tofighi, D. Schreurs, and J. T.-S. Horng, *Principles and Applications of RF/Microwave in Healthcare and Biosensing*. Academic Press, 2016.

[47] S. Jun and J. M. Irudayaraj, *Food Processing Operations Modeling: Design and Analysis, Second Edition*, vol. 107. CRC Press, 2008.

[48] Y. Oh and Y.-G. Koo, "Analysis of wave reflection from open-ended coaxial lines and application to the measurement of soil moisture and salinity," in *IEEE Antennas and Propagation Society International Symposium, 1998*, Atlanta, GA, 1998, vol. 4, pp. 2010–2013.

[49] H. Zheng and C. E. Smith, "Permittivity measurements using a short open-ended coaxial line probe," *IEEE Microw. Guid. Wave Lett.*, vol. 1, no. 11, pp. 337–339, Nov. 1991.

[50] D. Misra, M. Chabbra, B. R. Epstein, M. Microtznik, and K. R. Foster, "Noninvasive electrical characterization of materials at microwave frequencies using an open-ended coaxial line: test of an improved calibration technique," *IEEE Trans. Microw. Theory Techn.*, vol. 38, no. 1, pp. 8–14, Jan. 1990.

[51] E. C. Burdette, F. L. Cain, and J. Seals, "In Vivo Probe Measurement Technique for Determining Dielectric Properties at VHF through Microwave Frequencies," *IEEE Trans. Microw. Theory Techn.*, vol. 28, no. 4, pp. 414–427, Apr. 1980.

[52] A. Fornes-Leal, C. Garcia-Pardo, M. Frasson, V. Pons Beltrán, and N. Cardona, "Dielectric characterization of healthy and malignant colon tissues in the 0.5-18 GHz frequency band," *Phys. Med. Biol.*, vol. 61, no. 20, pp. 7334–7346, Oct. 2016.

[53] A. Kraszewski, M. A. Stuchly, S. S. Stuchly, and A. M. Smith, "In vivo and in vitro dielectric properties of animal tissues at radio frequencies," *Bioelectromagnetics*, vol. 3, no. 4, pp. 421–432, 1982.

[54] A. Peyman, A. A. Rezazadeh, and C. Gabriel, "Changes in the dielectric properties of rat tissue as a function of age at microwave frequencies," *Phys. Med. Biol.*, vol. 46, no. 6, pp. 1617–1629, Jun. 2001.

[55] J.-Z. Bao, S.-T. Lu, and W. D. Hurt, "Complex dielectric measurements and analysis of brain tissues in the radio and microwave frequencies," *IEEE Trans. Microw. Theory Techn.*, vol. 45, no. 10, pp. 1730–1741, Oct. 1997.

[56] M. C. Steel and R. J. Sheppard, "Dielectric properties of mammalian brain tissue between 1 and 18 GHz," *Phys. Med. Biol.*, vol. 30, no. 7, pp. 621–630, Jul. 1985.

[57] M. M. Brandy, S. A. Symons, and S. S. Stuchly, "Dielectric behavior of selected animal tissues in vitro at frequencies from 2 to 4 GHz," *IEEE Trans. Biomed. Eng.*, vol. 28, no. 3, pp. 305–307, Mar. 1981.

[58] M. Lazebnik, M. C. Converse, J. H. Booske, and S. C. Hagness, "Ultrawideband temperature-dependent dielectric properties of animal liver tissue in the microwave frequency range," *Phys. Med. Biol.*, vol. 51, no. 7, pp. 1941–1955, Apr. 2006.

[59] K. R. Foster, J. L. Schepps, R. D. Stoy, and H. P. Schwan, "Dielectric properties of brain tissue between 0.01 and 10 GHz," *Phys. Med. Biol.*, vol. 24, no. 6, pp. 1177–1187, Nov. 1979.

[60] D. Xu, L. Liu, and Z. Jiang, "Measurement of the Dielectric Properties of Biological Substances Using an Improved Open-Ended Coaxial Line Resonator Method," *IEEE Trans. Microw. Theory Techn.*, vol. 35, no. 12, pp. 1424–1428, Dec. 1987.

[61] J. A. Rogers, R. J. Sheppard, E. H. Grant, N. M. Bleehen, and D. J. Honess, "The dielectric properties of normal and tumour mouse tissue between 50 MHz and 10 GHz," *Br. J. Radiol.*, vol. 56, no. 665, pp. 335–338, May 1983.

[62] J.-L. Schwartz and G. A. R. Mealing, "Dielectric properties of frog tissues in vivo and in vitro," *Phys. Med. Biol.*, vol. 30, no. 2, pp. 117–124, Feb. 1985.

[63] R. A. Kleismit, G. Kozlowski, B. D. Foy, B. E. Hull, and M. Kazimierczuk, "Local complex permittivity measurements of porcine skin tissue in the frequency range from 1 GHz to 15 GHz by evanescent microscopy," *Phys. Med. Biol.*, vol. 54, no. 3, pp. 699–713, Feb. 2009.

[64] T. Sakai, K. Wake, S. Watanabe, and O. Hashimoto, "Temperature Compensation of Complex Permittivities of Biological Tissues and Organs in Quasi-Millimeter-Wave and Millimeter-Wave Bands," *J. Korean Inst. Electromagn. Eng. Sci.*, vol. 10, no. 4, pp. 231–236, Dec. 2010.

[65] J. L. Schepps and K. R. Foster, "The UHF and microwave dielectric properties of normal and tumour tissues: variation in dielectric properties with tissue water content," *Phys. Med. Biol.*, vol. 25, no. 6, pp. 1149–1159, Nov. 1980.

[66] D.-S. Yoo, "The dielectric properties of cancerous tissues in a nude mouse xenograft model," *Bioelectromagnetics*, vol. 25, no. 7, pp. 492–497, Oct. 2004.

[67] K. Sasaki, K. Wake, and S. Watanabe, "Measurement of the dielectric properties of the epidermis and dermis at frequencies from 0.5 GHz to 110 GHz," *Phys. Med. Biol.*, vol. 59, no. 16, pp. 4739–4747, Aug. 2014.

[68] A. Peyman *et al.*, "Variation in Dielectric Properties Due to

Pathological Changes in Human Liver," *Bioelectromagnetics*, vol. 36, no. 8, pp. 603–612, Dec. 2015.
[69] M. Lazebnik *et al.*, "A large-scale study of the ultrawideband microwave dielectric properties of normal breast tissue obtained from reduction surgeries," *Phys. Med. Biol.*, vol. 52, no. 10, pp. 2637–2656, May 2007.
[70] C. Polk and E. Postow, *Handbook of biological effects of electromagnetic fields*. CRC Press, 1996.
[71] C. Gabriel, "Dielectric properties of biological tissue: variation with age," *Bioelectromagnetics*, vol. 26, no. S7, pp. S12–S18, 2005.
[72] B. Mohammed, K. Bialkowski, A. Abbosh, P. C. Mills, and A. P. Bradley, "Dielectric properties of dog brain tissue measured in vitro across the 0.3-3 GHz band," *Bioelectromagnetics*, vol. 37, no. 8, pp. 549–556, Dec. 2016.
[73] M. A. Stuchly, A. Kraszewski, S. S. Stuchly, and A. M. Smith, "Dielectric properties of animal tissues in vivo at radio and microwave frequencies: comparison between species," *Phys. Med. Biol.*, vol. 27, no. 7, pp. 927–936, Jul. 1982.
[74] A. Peyman and C. Gabriel, "Dielectric properties of porcine glands, gonads and body fluids," *Phys. Med. Biol.*, vol. 57, no. 19, pp. N339–N344, Oct. 2012.
[75] E. S. Nadimi *et al.*, "In vivo and in situ measurement and modelling of intra-body effective complex permittivity," *Healthc. Technol. Lett.*, vol. 2, no. 6, pp. 135–140, Nov. 2015.
[76] K. O. Olawale, R. J. Petrell, D. G. Michelson, and A. W. Trites, "The dielectric properties of the cranial skin of five young captive Steller sea lions (Eumetopias jubatus), and a similar number of young domestic pigs (Sus scrofa) and sheep (Ovis aries) between 0.1 and 10 GHz," *Physiol. Meas.*, vol. 26, no. 5, pp. 627–637, Oct. 2005.
[77] J. Cho *et al.*, "In-vivo measurements of the dielectric properties of breast carcinoma xenografted on nude mice," *Int. J. Cancer*, vol. 119, no. 3, pp. 593–598, Aug. 2006.
[78] S. Gabriel, R. W. Lau, and C. Gabriel, "The dielectric properties of biological tissues: II. Measurements in the frequency range 10 Hz to 20 GHz," *Phys. Med. Biol.*, vol. 41, no. 11, pp. 2251–2269, Nov. 1996.
[79] A. P. O'Rourke *et al.*, "Dielectric properties of human normal, malignant and cirrhotic liver tissue: in vivo and ex vivo measurements from 0.5 to 20 GHz using a precision open-ended coaxial probe.," *Phys. Med. Biol.*, vol. 52, no. 15, pp. 4707–4719, Aug. 2007.
[80] A. Vander Vorst, A. Rosen, and Y. Kotsuka, *RF/Microwave Interaction with Biological Tissues*. John Wiley & Sons, 2006.
[81] K. R. Foster and H. P. Schwan, "Dielectric properties of tissues and biological materials: a critical review," *Crit. Rev. Biomed. Eng.*, vol. 17, no. 1, pp. 25–104, Jan. 1989.
[82] M.-C. Gosselin *et al.*, "Development of a new generation of high-resolution anatomical models for medical device evaluation: the Virtual Population 3.0," *Phys. Med. Biol.*, vol. 59, no. 18, pp. 5287–5303, Sep. 2014.
[83] "The Visible Human Project®." [Online]. Available: https://www.nlm.nih.gov/research/visible/visible_human.html. [Accessed: 18-Apr-2017].
[84] T. Wu *et al.*, "Chinese adult anatomical models and the application in evaluation of RF exposures," *Phys. Med. Biol.*, vol. 56, no. 7, pp. 2075–2089, Apr. 2011.
[85] N. Petoussi-Henss, M. Zanki, U. Fill, and D. Regulla, "The GSF family of voxel phantoms," *Phys. Med. Biol.*, vol. 47, no. 1, pp. 89–106, Jan. 2002.
[86] T. Nagaoka *et al.*, "Development of realistic high-resolution whole-body voxel models of Japanese adult males and females of average height and weight, and application of models to radio-frequency electromagnetic-field dosimetry," *Phys. Med. Biol.*, vol. 49, no. 1, pp. 1–15, Jan. 2004.
[87] P. Dimbylow, "Development of the female voxel phantom, NAOMI, and its application to calculations of induced current densities and electric fields from applied low frequency magnetic and electric fields," *Phys. Med. Biol.*, vol. 50, no. 6, pp. 1047–1070, Mar. 2005.
[88] P. J. Dimbylow, "FDTD calculations of the whole-body averaged SAR in an anatomically realistic voxel model of the human body from 1 MHz to 1 GHz," *Phys. Med. Biol.*, vol. 42, no. 3, pp. 479–490, Mar. 1997.
[89] "CST STUDIO SUITE®," *CST AG, Germany*. [Online]. Available: www.cst.com.
[90] P. Stavroulakis, *Biological Effects of Electromagnetic Fields*. Springer, 2003.
[91] S. Romeo *et al.*, "Dielectric Characterization Study of Liquid-Based Materials for Mimicking Breast Tissues," *Microw. Opt. Technol. Lett.*, vol. 53, no. 6, pp. 1276–1280, Jun. 2011.
[92] X. Li, S. K. Davis, S. C. Hagness, D. W. Van Der Weide, and B. D. Van Veen, "Microwave imaging via space-time beamforming: Experimental investigation of tumor detection in multilayer breast phantoms," *IEEE Trans. Microw. Theory Techn.*, vol. 52, no. 8, pp. 1856–1865, Aug. 2004.
[93] S. Castelló-Palacios, C. Garcia-Pardo, A. Fornes-Leal, N. Cardona, and A. Vallés-Lluch, "Wideband Phantoms of Different Body Tissues for Heterogeneous Models in Body Area Networks," in *2017 39th Annual International Conference of the IEEE Engineering in Medicine and Biology Society (EMBC)*, Jeju, 2017, pp. 3032–3035.
[94] M. Lazebnik, E. L. Madsen, G. R. Frank, and S. C. Hagness, "Tissue-mimicking phantom materials for narrowband and ultrawideband microwave applications," *Phys. Med. Biol.*, vol. 50, no. 18, pp. 4245–4258, Sep. 2005.
[95] K. Ito, "Human Body Phantoms for Evaluation of Wereable and Implantable Antennas," in *The Second European Conference on Antennas and Propagation, EuCAP 2007*, Edinburgh, 2007, pp. 1–6.
[96] A. Abu Bakar, A. Abbosh, P. Sharpe, M. E. Bialkowski, and Y. Wang, "Heterogeneous Breast Phantom for Ultra Wideband Microwave Imaging," *Microw. Opt. Technol. Lett.*, vol. 53, no. 7, pp. 1595–1598, Jul. 2011.
[97] A. A. Bakar, A. Abbosh, and M. Bialkowski, "Fabrication and Characterization of a Heterogeneous Breast Phantom for Testing an Ultrawideband Microwave Imaging System," in *Asia-Pacific Microwave Conference 2011*, Melbourne, VIC, 2011, pp. 1414–1417.
[98] T. Yilmaz, R. Foster, and Y. Hao, "Broadband Tissue Mimicking Phantoms and a Patch Resonator for Evaluating Noninvasive Monitoring of Blood Glucose Levels," *IEEE Trans. Antennas Propag.*, vol. 62, no. 6, pp. 3064–3075, Jun. 2014.
[99] Y. Baskharoun, A. Trehan, N. K. Nikolova, and M. D. Noseworthy, "Physical phantoms for microwave imaging of the breast," in *2012 IEEE Topical Conference on Biomedical Wireless Technologies, Networks, and Sensing Systems (BioWireleSS)*, Santa Clara, CA, 2012, pp. 73–76.
[100] S. Alshehri, A. Jantan, R. S. A. Raja Abdullah, R. Mahmud, S. Khatun, and Z. Awang, "A UWB imaging system to detect early breast cancer in heterogeneous breast phantom," in *International Conference on Electrical, Control and Computer Engineering 2011 (InECCE)*, Pahang, 2011, pp. 238–242.
[101] I. J. Youngs, A. S. Treen, G. Fixter, and S. Holden, "Design of solid broadband human tissue simulant materials," *IEE Proc. - Sci. Meas. Technol.*, vol. 149, no. 6, pp. 323–328, Nov. 2002.
[102] J. Bourqui, M. A. Campbell, T. Williams, and E. C. Fear, "Antenna evaluation for ultra-wideband microwave imaging," *Int. J. Antennas Propag.*, vol. 2010, pp. 1–8, 2010.
[103] J. Garrett and E. Fear, "Stable and flexible materials to mimic the dielectric properties of human soft tissues," *IEEE Antennas Wirel. Propag. Lett.*, vol. 13, pp. 599–602, Mar. 2014.
[104] P. Prakash, M. C. Converse, D. M. Mahvi, and J. G. Webster, "Measurement of the specific heat capacity of liver phantom," *Physiol. Meas.*, vol. 27, no. 10, pp. N41–N46, Oct. 2006.
[105] W. C. Khor, F. Y. Hui, M. E. Bialkowski, and S. Crozier, "Investigations into microwave properties of various substances to develop a breast phantom for a UWB breast tumour radar detecting system," in *MIKON 2008 - 17th International Conference on Microwaves, Radar and Wireless Communications*, Wroclaw, 2008, pp. 1–4.
[106] A. R. Guraliuc, M. Zhadobov, O. De Sagazan, and R. Sauleau, "Solid Phantom for Body-Centric Propagation Measurements at 60 GHz," *IEEE Trans. Microw. Theory Techn.*, vol. 62, no. 6, pp. 1373–1380, Jun. 2014.
[107] C. Gabriel, "Tissue Equivalent Material for Hand Phantoms," *Phys. Med. Biol.*, vol. 52, no. 14, pp. 4205–4210, Jun. 2007.
[108] H. Yamamoto, J. Zhou, and T. Kobayashi, "Ultra wideband electromagnetic phantoms for antennas and propagation studies," *IEICE Trans. Fundam. Electron. Commun. Comput. Sci.*, vol. E91–A, no. 11, pp. 3173–3182, 2008.
[109] D. Andreuccetti, R. Fossi, and C. Petrucci, "Calculation of the Dielectric Properties of Body Tissues." [Online]. Available: http://niremf.ifac.cnr.it/tissprop/htmlclie/htmlclie.php.
[110] N. Chahat, M. Zhadobov, and R. Sauleau, "Broadband Tissue-Equivalent Phantom for BAN Applications at Millimeter Waves," *IEEE Trans. Microw. Theory Techn.*, vol. 60, no. 7, pp. 2259–2266, Jul.

2012.
[111] M. Saviz and R. Faraji-Dana, "A Theoretical Model for the Frequency-Dependent Dielectric Properties of Corneal Tissue at Microwave Frequencies," *Prog. Electromagn. Res.*, vol. 137, pp. 389–406, 2013.
[112] C.-K. Chou, G.-W. Chen, A. W. Guy, and K. H. Luk, "Formulas for preparing phantom muscle tissue at various radiofrequencies," *Bioelectromagnetics*, vol. 5, no. 4, pp. 435–441, 1984.
[113] S. Oh, Y.-C. Ryu, G. Carluccio, C. T. Sica, and C. M. Collins, "Measurement of SAR-induced temperature increase in a phantom and in vivo with comparison to numerical simulation," *Magn. Reson. Med.*, vol. 71, no. 5, pp. 1923–1931, May 2014.
[114] Y. Wang, A. M. Abbosh, B. Henin, and P. T. Nguyen, "Synthetic bandwidth radar for ultra-wideband microwave imaging systems," *IEEE Trans. Antennas Propag.*, vol. 62, no. 2, pp. 698–705, Feb. 2014.
[115] P. Homolka *et al.*, "Design of a head phantom produced on a 3D rapid prototyping printer and comparison with a RANDO and 3M lucite head phantom in eye dosimetry applications," *Phys. Med. Biol.*, vol. 62, no. 8, pp. 3158–3174, Apr. 2017.
[116] D. Kurup, W. Joseph, G. Vermeeren, and L. Martens, "Path loss model for in-body communication in homogeneous human muscle tissue," *Electron. Lett.*, vol. 45, no. 9, pp. 453–454, Apr. 2009.
[117] G. Iddan, G. Meron, A. Glukhovsky, and P. Swain, "Wireless capsule endoscopy.," *Nature*, vol. 405, no. 6785, pp. 417–418, May 2000.
[118] H.-D. Lin, A.-N. Khripkov, D. V. Vlasov, and T.-H. Tao, "Using ultra-wideband sensing technology for intestinal motility measurement," in *2010 5th Cairo International Biomedical Engineering Conference*, Cairo, 2010, pp. 45–48.
[119] H. Burri and D. Senouf, "Remote monitoring and follow-up of pacemakers and implantable cardioverter defibrillators," *Europace*, vol. 11, no. 6, pp. 701–709, Jun. 2009.
[120] J. Liang, L. Guo, C. C. Chiau, and X. Chen, "CPW-fed circular disc monopole antenna for UWB applications," in *2005 IEEE International Workshop on Antenna Technology Small Antennas and Novel Metamaterials (iWAT)*, Singapore, 2005, pp. 505–508.
[121] E. G. Lim *et al.*, "Transmitter antennas for wireless capsule endoscopy," in *2012 International SoC Design Conference (ISOCC)*, Jeju Island, 2012, pp. 269–272.
[122] C. A. Balanis, *Antenna Theory: Analysis and Design*, 3rd ed. New York: John Wiley & Sons, 2005.
[123] K. Y. Yazdandoost and R. Miura, "Miniaturized UWB implantable Antenna for Brain-Machine-Interface," in *2015 9th European Conference on Antennas and Propagation (EuCAP)*, Lisbon, 2015, pp. 1–5.
[124] Q. Wang, K. Wolf, and D. Plettemeier, "An UWB capsule endoscope antenna design for biomedical communications," in *2010 3rd International Symposium on Applied Sciences in Biomedical and Communication Technologies (ISABEL 2010)*, Rome, 2010, pp. 1–6.
[125] Q. Wang, D. Plettemeier, C. Andreu, C. Garcia-Pardo, and N. Cardona, "Characteristics comparison of three different WCE implanted antennas in UWB low band," in *Proceedings of the 11th EAI International Conference on Body Area Networks*, Turin, 2016, pp. 8–9.
[126] C. Andreu, C. Garcia-Pardo, A. Fornes-Leal, M. Cabedo-Fabrés, and N. Cardona, "UWB In-Body Channel Performance by Using a Direct Antenna Designing Procedure," in *11th European Conference on Antennas and Propagation (EUCAP)*, 2017, pp. 278–282.
[127] C. Andreu, C. Garcia-Pardo, A. Fornes-Leal, M. Cabedo-Fabrés, and N. Cardona, "UWB In-Body Channel Performance by Using a Direct Antenna Designing Procedure," in *2017 11th European Conference on Antennas and Propagation (EuCAP)*, Paris, 2017, pp. 1–4.
[128] Q. Wang, R. Hahnel, H. Zhang, and D. Plettemeier, "On-body directional antenna design for in-body UWB wireless communication," in *2012 6th European Conference on Antennas and Propagation (EUCAP)*, Prague, 2012, pp. 1011–1015.
[129] L. A. Yimdjo Poffelie, P. J. Soh, S. Yan, and G. A. E. Vandenbosch, "A High-Fidelity All-Textile UWB Antenna With Low Back Radiation for Off-Body WBAN Applications," *IEEE Trans. Antennas Propag.*, vol. 64, no. 2, pp. 757–760, Feb. 2016.
[130] S. Kang and C. W. Jung, "Wearable Fabric Reconfigurable Beam-Steering Antenna for On/Off-Body Communication System," *Int. J. Antennas Propag.*, vol. 2015, pp. 1–7, 2015.
[131] W. Jeong and J. Choi, "A low profile IR-UWB antenna with conical radiation pattern for on-body communications," in *2015 IEEE International Symposium on Antennas and Propagation & USNC/URSI National Radio Science Meeting*, Vancouver, BC, 2015, pp. 2023–2024.
[132] A. Khaleghi, I. Balasingham, and R. Chávez-Santiago, "An ultra-wideband wire spiral antenna for in-body communications using different material matching layers," in *2014 36th Annual International Conference of the IEEE Engineering in Medicine and Biology Society*, Chicago, IL, 2014, pp. 6985–6988.
[133] E. Miralles, C. Andreu, M. Cabedo-Fabrés, M. Ferrando-Bataller, and J. F. Monserrat, "UWB On-body Slotted Patch Antennas for In-Body Communications," in *2017 11th European Conference on Antennas and Propagation (EUCAP)*, Paris, 2017, pp. 167–171.
[134] C. Andreu, S. Castelló-Palacios, C. Garcia-Pardo, A. Fornes-Leal, A. Vallés-Lluch, and N. Cardona, "Spatial In-Body Channel Characterization Using an Accurate UWB Phantom," *IEEE Trans. Microw. Theory Techn.*, vol. 64, no. 11, pp. 3995–4002, Nov. 2016.
[135] S. Støa, R. Chávez-Santiago, and I. Balasingham, "An ultra wideband communication channel model for the human abdominal region," in *2010 IEEE Globecom Workshops*, Miami, FL, 2010, pp. 246–250.
[136] A. Khaleghi, R. Chávez-Santiago, and I. Balasingham, "Ultra-wideband statistical propagation channel model for implant sensors in the human chest," *IET Microwaves, Antennas Propag.*, vol. 5, no. 15, pp. 1805–1812, Dec. 2011.
[137] M. Kanaan and M. Suveren, "A novel frequency-dependent path loss model for ultra wideband implant body area networks," *Meas. J. Int. Meas. Confed.*, vol. 68, pp. 117–127, May 2015.
[138] Y. Shimizu, T. Furukawa, D. Anzai, and J. Wang, "Performance improvement by transmit diversity technique for implant ultra-wideband communication," *IET Microwaves, Antennas Propag.*, vol. 10, no. 10, pp. 1106–1112, 2016.
[139] J. Shi and J. Wang, "Channel characterization and diversity feasibility for in-body to on-body communication using low-band UWB signals," in *2010 3rd International Symposium on Applied Sciences in Biomedical and Communication Technologies (ISABEL 2010)*, Rome, 2010, pp. 1–4.
[140] K. M. S. Thotahewa, J.-M. Redoutè, and M. R. Yuce, "Propagation, Power Absorption, and Temperature Analysis of UWB Wireless Capsule Endoscopy Devices Operating in the Human Body," *IEEE Trans. Microw. Theory Techn.*, vol. 63, no. 11, pp. 3823–3833, Nov. 2015.
[141] K. Y. Yazdandoost, K. Takizawa, and R. Miura, "UWB antenna and propagation for wireless endoscopy," in *2014 IEEE 25th Annual International Symposium on Personal, Indoor, and Mobile Radio Communication (PIMRC)*, Washington DC, 2014, pp. 2155–2159.
[142] S. Gezici *et al.*, "Localization via ultra-wideband radios: a look at positioning aspects for future sensor networks," *IEEE Signal Process. Mag.*, vol. 22, no. 4, pp. 70–84, Jul. 2005.
[143] B. Moussakhani, J. T. Flåm, S. Støa, I. Balasingham, and T. Ramstad, "On localisation accuracy inside the human abdomen region," *IET Wirel. Sens. Syst.*, vol. 2, no. 1, pp. 9–15, Mar. 2012.
[144] J. Shi, D. Anzai, and J. Wang, "Channel Modeling and Performance Analysis of Diversity Reception for Implant UWB Wireless Link," *IEICE Trans. Commun.*, vol. E95.B, no. 10, pp. 3197–3205, Oct. 2012.
[145] M. Marinova *et al.*, "Diversity Performance of Off-Body MB-OFDM UWB-MIMO," *IEEE Trans. Antennas Propag.*, vol. 63, no. 7, pp. 3187–3197, Jul. 2015.